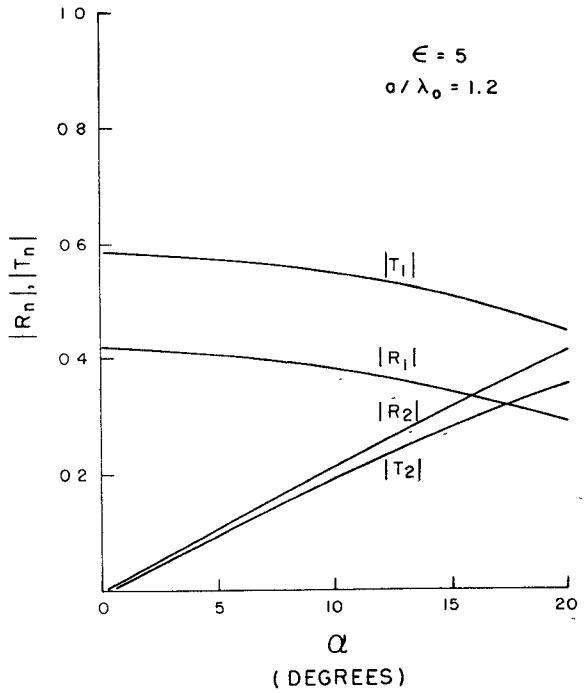

Fig. 4. Amplitudes of first two propagating modes in each medium as a function of slant angle α. TE_{10} mode incidence with $a/\lambda_0 = 1.2$ is assumed.

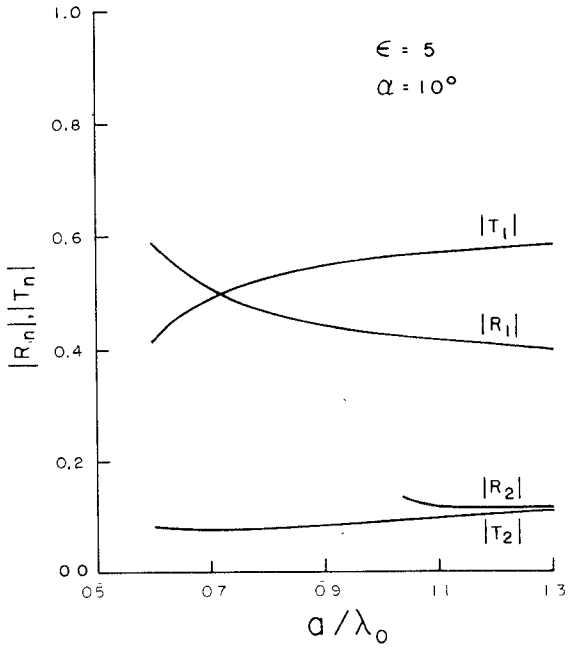

Fig. 5. Amplitudes of first two propagating modes in each medium as a function of a/λ_0.

ACKNOWLEDGMENT

The author wishes to thank Dr. R. A. Hurd for many valuable discussions and Dr. Y. L. Chow for providing the numerical data for comparison. The author also wishes to thank Mrs. M. Steen for doing the computations.

REFERENCES

[1] Y. L. Chow and S. C. Wu, "A moment method with mixed basis functions for scatterings by waveguide junctions," *IEEE Trans. Microwave Theory Tech.*, vol. MTT-21, pp. 333–340, May 1973.
[2] G. De Jong and W. Offringa, "Reflection and transmission by a slant interface between two media in a waveguide," *Int. J. Electron.*, vol. 34, pp. 453–463, 1973.

The Relations between Scalar Modes in a Lenslike Medium and Vector Modes in a Self-Focusing Optical Fiber

G. L. YIP, MEMBER, IEEE, AND S. NEMOTO

***Abstract*—The relations are established between the scalar modes in an infinite lenslike medium and the vector modes in a self-focusing optical fiber with a finite homogeneous cladding. It is shown that both the transverse fields and the longitudinal fields of the vector modes can be expressed in terms of the scalar modes provided the fiber is operated in the core mode region. Otherwise, significant discrepancies could arise. The scalar modes, however, cannot describe the cladding modes which are caused by the index discontinuity at the outer surface of the cladding.**

I. INTRODUCTION

In integrated and fiber optics many problems involve a medium with an inhomogeneous refractive index. When one is confronted with a problem related to a self-focusing optical fiber, it is essential to know its propagation characteristics. The inhomogeneous nature of this fiber makes its properties more difficult to analyze than the fiber with a homogeneous core. The simplest model of the self-focusing fiber is that of an infinite lenslike medium. For this medium many studies have been carried out using ray-optical method, wave-optics method, and vector field analysis [1], [2]. In particular, the wave-optics method yields the scalar modes. The numerical methods for computing the propagation characteristics of self-focusing fibers with an infinite homogeneous cladding were employed by several authors [3], [4]. Most recently, the numerical method based on an earlier work of Vigants [5] was applied to the more realistic self-focusing fiber with a finite homogeneous cladding [4], [6].

Since the scalar modes can be expressed in analytic functions, it is, in many situations, convenient to approximate the vector modes in the self-focusing fiber by the scalar modes whenever possible. Before doing this, however, it is necessary to understand the relations between the scalar and vector modes and the extent to which the scalar-mode approximation is valid. So far nothing has been reported on this subject. The purpose of this short paper is to establish the relations between the scalar modes in an infinite lenslike medium and the vector modes in a self-focusing fiber with a finite homogeneous cladding, and to show the limitations of the scalar-mode approximation. For this purpose the various propagation characteristics of the scalar modes are compared with those of the vector modes obtained by the numerical method [4], [6].

II. THE SCALAR MODES IN A LENSLIKE MEDIUM

In a cylindrical coordinate system (r,θ,z) the refractive index distribution of the fiber is assumed to be

$$n(r) = \begin{cases} n_0[1 - \Delta(r/a)^2], & 0 \le r \le a \\ n_0(1 - \Delta), & a \le r < b \\ n_3, & b < r < \infty \end{cases} \quad (1)$$

where a and b are the inner and outer radii of cladding, and $0 < \Delta \ll 1$. Let us consider an infinite lenslike medium whose index distribution is expressed as

$$\hat{n}(r) = n_0[1 - (r/d)^2]^{1/2}. \quad (2)$$

The index variation in the core region of the fiber is well approxi-

Manuscript received April 2, 1974; revised September 9, 1974. This work was supported by the Defence Research Board and National Research Council of Canada.
The authors are with the Department of Electrical Engineering, McGill University, Montreal, P.Q., Canada.

mated by $\hat{n}(r)$ if we make $d = a/(2\Delta)^{1/2}$. The scalar modes in this medium are given by [7], [8] (time dependence exp $(j\omega t)$ is assumed)

$$\begin{Bmatrix} U_{nm}{}^{c} \\ U_{nm}{}^{s} \end{Bmatrix} = \psi_{nm(r)} \begin{Bmatrix} \cos n\theta \\ \sin n\theta \end{Bmatrix} \exp(-j\beta_{nm}z) \tag{3}$$

$$\psi_{nm}(r) = \frac{1}{s_0}\left(\frac{m!}{\pi(n+m)!}\right)^{1/2}\left(\frac{r}{s_0}\right)^{n} L_m{}^{n}\left(\frac{r^2}{s_0{}^2}\right)\exp\left[-(1/2)(r/s_0)^2\right] \tag{4}$$

$$\beta_{nm}{}^2 = (n_0k_0)^2 - 2(n + 2m + 1)/s_0{}^2 \tag{5}$$

where $s_0 = (d/n_0k_0)^{1/2}$, n and m are nonnegative integers, $k_0 = 2\pi/\lambda_0$ is the wavenumber in free space, and $L_m{}^{n}(x) = (e^{x}x^{-n}/m!)\cdot(d^m/dx^m)(e^{-x}x^{n+m})$ is the generalized Laguerre polynomials. s_0 is called the characteristic spot size of the medium and is expressed as $s_0{}^2 = a/n_0k_0(2\Delta)^{1/2}$ by using $d = a/(2\Delta)^{1/2}$. Hereafter, β_{nm}/k_0 and $(\partial\beta_{nm}/\partial k_0)^{-1}$ are referred to as the normalized propagation constant and the normalized group velocity of the scalar nm modes ($U_{nm}{}^{c}$ or $U_{nm}{}^{s}$), and k_0a as the normalized frequency.

III. COMPARISONS OF THE VARIOUS CHARACTERISTICS

In Fig. 1, the normalized propagation constants of several scalar modes are compared with those of the vector modes in the fiber with a finite cladding obtained by the numerical method [4], [6]. The paired numbers in this figure correspond to the mode numbers (nm) of the scalar modes (this applies also to Figs. 2 and 3) and U represents either β_{nm}/k_0 or β/k_0, where β is the propagation constant of the vector modes. In Fig. 1(a)[1] the results for the infinite-cladding approximation obtained by the numerical method [4], [6] are also shown for comparison. Note that, considering the finite core radius, the cutoff conditions for the scalar modes are given by [9] $\beta_{nm}/k_0 = n_0(1 - \Delta) = 1.5$. Hence, for the scalar modes, the normalized propagation constants less than 1.5 have physical meaning only when we consider an infinite lenslike medium. It is seen from Fig. 1(a) that, far from cutoff, the three propagation constants cannot be distinguished. While the propagation constants for the infinite-cladding approximation terminate in $U = 1.5$ as cutoff points, the propagation constants of the scalar modes are close to those of the vector modes in the fiber with a finite cladding. However, as seen from Fig. 1(b), the propagation constants of the scalar modes deviate remarkably from those of the vector modes when k_0a is small.

In Fig. 2 the normalized group velocities of several scalar modes are compared with those of the vector modes obtained by the numerical method [6] (v_g/c, where c is the light velocity in free space, represents either $(\partial\beta_{nm}/\partial k_0)^{-1}$ or $(\partial\beta/\partial k_0)^{-1}$). In this figure the results for the infinite-cladding approximation are also shown [6]. While the infinite-cladding approximation does not give a correct variation of group velocities with frequency for small values of k_0a, the group velocities of the scalar modes are similar in variation to those of the vector modes in the fiber with a finite cladding. From these figures alone, however, we cannot obtain enough information to establish the relation between the scalar and vector modes. Therefore, the radial field distributions of several scalar modes are compared with those of the vector modes. This comparison was done in two cases where 1) $U = 1.30$ and 2) $U = 1.5105$ or 1.517. Cases 1) and 2) correspond to the cladding mode region and the core mode region, respectively.

In Fig. 3 the radial field distributions of several scalar modes are compared with the transverse electric fields of the vector modes obtained by the numerical method [6]. In this figure the longitudinal fields obtained from the scalar-mode approximation are also compared with those of the vector modes (see the following sections). Since all the electric-field components of the vector modes are normalized by the maximum values of E_r, the fields of the scalar modes are also normalized by their maximum values. In case 1), the scalar fields deviate remarkably from the vector fields, corresponding to the notable discrepancies between the propagation constants of the scalar and vector modes [Fig. 1(b)]. In case 2), especially when $U = 1.517$, the scalar fields are hardly distinguishable from the vector fields.

[1] For the vector modes in the fiber with a finite cladding, the values of the parameters are the same as in Ahmew [6]. This applies also to Figs. 2, 3, and 5.

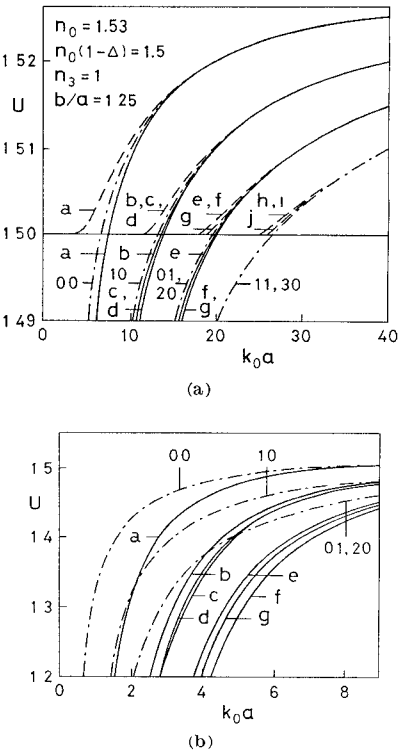

Fig. 1. Normalized propagation constant U versus normalized frequency k_0a. — for the fiber with a finite cladding obtained by the numerical method. - - - infinite-cladding approximation obtained by the numerical method. -·- scalar-mode approximation (5). *a*—HE_{11}; *b*—TE_{01}; *c*—TM_{01}; *d*—HE_{21}; *e*—EH_{11}; *f*—HE_{12}; *g*—HE_{31}; *h*—TE_{02}; *i*—TM_{02}; *j*—EH_{21}.

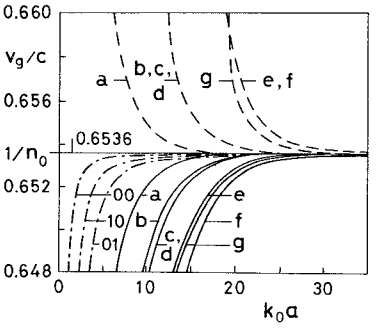

Fig. 2. Normalized group velocity v_g/c versus normalized frequency. — for the fiber with a finite cladding obtained by the numerical method. - - - infinite-cladding approximation obtained by the numerical method. -·- scalar-mode approximation. *a*—HE_{11}; *b*—TE_{01}; *c*—TM_{01}; *d*—HE_{21}; *e*—EH_{11}; *f*—HE_{12}; *g*—HE_{31}.

IV. RELATIONS BETWEEN THE SCALAR AND VECTOR MODES

It is seen from Fig. 3 that, far from cutoff, the fields of the vector modes are tightly bound to the core and have negligibly small amplitudes in the cladding. Therefore, the fiber can be regarded as an infinite lenslike medium when it is operated in the core mode region. According to the vector-field analysis [1], the transverse fields of the hybrid modes in an infinite lenslike medium of (2) are given by

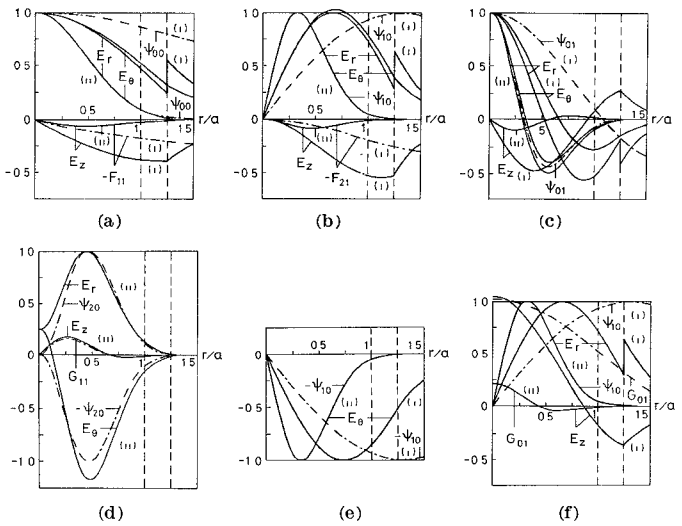

Fig. 3. Radial field distributions of the scalar and vector modes. — the electric fields of the vector modes in the fiber with a finite cladding obtained by the numerical method. –– the fields of the scalar modes. (4) and (19). (a) 00 – HE_{11}. (b) 10 – HE_{21}. (c) 01 – HE_{12}. (d) 20 – EH_{11}. (e) 10 – TE_{01}. (f) 10 – TM_{01}. (i) $U = 1.30$, (ii) $U = 1.5105$ for (c) and (d); $U = 1.517$ for (a), (b), (e), and (f). Two broken lines in each figure indicate the positions of the inner and outer surfaces of the cladding.

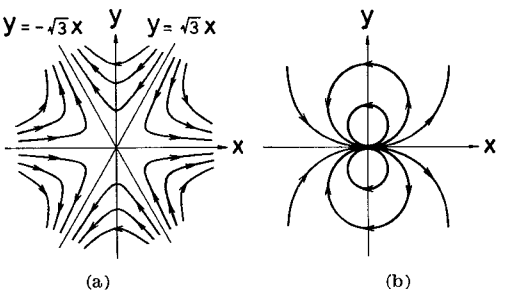

Fig. 4. Electric-field structures of the (a) HE_{31} and (b) EH_{11} modes.

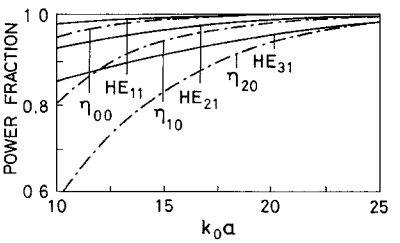

Fig. 5. Fraction of power in the core. — for the fiber with a finite cladding obtained by the numerical method. –– scalar-mode approximation: (16).

$$\boldsymbol{E}^{(i)} = (\mp j\boldsymbol{i}_r - \boldsymbol{i}_\theta)\Psi_i, \qquad \boldsymbol{H}^{(i)} = n_0 Y_0 \boldsymbol{i}_z \times \boldsymbol{E}^{(i)} \tag{6}$$

$$\Psi_i = c_i \left(\frac{r}{s_0}\right)^{n\mp 1} L_{m-1}^{n\mp 1}\left(\frac{r^2}{s_0^2}\right) \exp\left[-(1/2)(r/s_0)^2\right], \quad i = 1,2 \tag{7}$$

$$\begin{Bmatrix}\beta_1^2 \\ \beta_2^2\end{Bmatrix} = (n_0 k_0)^2 - 2\left(n + 2\begin{Bmatrix} m-1 \\ m \end{Bmatrix}\right) \Big/ s_0^2 \tag{8}$$

where $n = 1,2,3,\cdots$, $m = 1,2,3,\cdots$, $\boldsymbol{i}_r$, $\boldsymbol{i}_\theta$, and $\boldsymbol{i}_z$ are the unit vectors in the r, θ, and z directions, respectively, the θ and z dependences of the fields are assumed to be $\exp(-jn\theta)$ and $\exp(-j\beta_i z)$, and the upper (lower) sign corresponds to $i = 1$ ($i = 2$) [this applies also to (9) and (10)]. c_i are the constants and Y_0 is the intrinsic admittance of free space. By adding the θ and z-dependent factors to the first equation of (6) and producing the real functions of θ, the r and θ components of the electric fields are expressed as

$$\begin{Bmatrix} E_r^{(i)} \\ E_\theta^{(i)} \end{Bmatrix} = \Psi_i \begin{Bmatrix} \cos n\theta \\ \mp \sin n\theta \end{Bmatrix} \exp(-j\beta_i z), \qquad i = 1,2. \tag{9}$$

It can be shown [6] that, far from cutoff, the transverse electric fields of the hybrid modes in the fiber take the same form as (9) with Ψ_i and β_i replaced by the unknown functions, namely the HE (EH) modes have the same form as (9) with $i = 1$ ($i = 2$). In fact, from (27) and (28) in [1], the following relations are obtained:

$$E_z^{(i)}/H_z^{(i)} = \pm(n_0 Y_0)^{-1} \cos n\theta / \sin n\theta, \qquad i = 1,2. \tag{10}$$

Therefore, $i = 1$ ($i = 2$) corresponds to the HE (EH) modes [10]. From (4), (5), (7), and (8) it follows that

$$\Psi_1 \propto \Psi_{pq}, \qquad \beta_1 = \beta_{pq} \tag{11}$$

$$\Psi_2 \propto \Psi_{tq}, \qquad \beta_2 = \beta_{tq} \tag{12}$$

where $p = n - 1$, $q = m - 1$, and $t = n + 1$. These relations were pointed out also by Kurtz [11]. It is seen from Figs. 1 and 3 that, far from cutoff, the radial field distributions and propagation constants of the HE_{11}, HE_{12}, HE_{21}, and HE_{31} modes satisfy (11) and those of the EH_{11} and EH_{21} modes satisfy (12). Therefore, we can conclude that, far from cutoff, the HE_{nm} modes in the fiber correspond to the scalar pq modes and the EH_{nm} modes correspond to the scalar tq modes. Similar investigations on the TE and TM modes yield the following relations when the fiber is operated in the core mode region:

$$\begin{Bmatrix} E_\theta \\ E_r \end{Bmatrix} \simeq \mp \Psi_{1q}(r) \exp(-j\beta_{1q} z) \tag{13}$$

where the upper (lower) equation is applied to the TE_{0m} (TM_{0m}) modes[2] and $q = m - 1$. Note that $E_r = 0$ ($E_\theta = 0$) for the TE (TM) modes. For the transverse magnetic fields it was confirmed from the numerical results [6] that, far from cutoff, the same relation as the second equation of (6) holds approximately for the HE, EH, TE, and TM modes.

To summarize, when the fiber is operated in the core mode region, the transverse electric fields of the vector modes are expressed approximately as follows:

$$\begin{aligned} \boldsymbol{E}_{nm}^{\mathrm{HE}} &= U_{pq}{}^c\boldsymbol{i}_x - U_{pq}{}^s\boldsymbol{i}_y, & \boldsymbol{E}_{nm}^{\mathrm{EH}} &= U_{tq}{}^c\boldsymbol{i}_x + U_{tq}{}^s\boldsymbol{i}_y \\ \boldsymbol{E}_{0m}^{\mathrm{TE}} &= U_{1q}{}^s\boldsymbol{i}_x - U_{1q}{}^c\boldsymbol{i}_y, & \boldsymbol{E}_{0m}^{\mathrm{TM}} &= U_{1q}{}^c\boldsymbol{i}_x + U_{1q}{}^s\boldsymbol{i}_y \end{aligned} \tag{14}$$

where $\boldsymbol{i}_x$ and $\boldsymbol{i}_y$ are the unit vectors of x and y directions in the rectangular coordinate system (x,y,z). Equation (14) is obtained from (3), (9), (11)–(13), and the relation between the rectangular and cylindrical components of the field. For example, from (3) and (14) it follows that

$$\begin{Bmatrix} \boldsymbol{E}_{31}^{\mathrm{HE}} \\ \boldsymbol{E}_{11}^{\mathrm{EH}} \end{Bmatrix} = \Psi_{20}(r)(\boldsymbol{i}_x \cos\theta \mp \boldsymbol{i}_y \sin\theta) \exp(-j\beta_{20} z). \tag{15}$$

Hence, far from cutoff, the r and z dependences of the HE_{31} and EH_{11} modes are almost the same. But, as shown in Fig. 4, these modes differ appreciably in their field structures. The fraction η of power carried in the core is defined as the ratio of the energy passing through a transverse plane at z = constant within the core to the energy passing through the entire plane at z = constant. For the HE_{nm} modes η is given by

$$\eta \simeq \eta_{pq} = 2\pi \int_0^a \Psi_{pq}{}^2 r\, dr \tag{16}$$

from (3), (4), and (14). In Fig. 5, η_{pq} are compared with the power fraction obtained numerically [6] for several modes. It is seen that agreement also can be recognized when $k_0 a$ is large.

[2] The ($\mp$) signs in (13) have no physical significance and were introduced only for the convenience of expression [see (14)].

V. EXPRESSIONS FOR THE LONGITUDINAL FIELDS

From Maxwell's equations and (6), (7), (9), (11), and (12), the longitudinal components of the fields are given by

$$\begin{Bmatrix} E_{z,nm} \\ ZH_{z,nm} \end{Bmatrix} \simeq jF_{nm}(r) \begin{Bmatrix} \cos n\theta \\ \sin n\theta \end{Bmatrix} \exp(-j\beta_{pq}z) \tag{17}$$

$$\begin{Bmatrix} E_{z,nm} \\ ZH_{z,nm} \end{Bmatrix} \simeq jG_{nm}(r) \begin{Bmatrix} -\cos n\theta \\ \sin n\theta \end{Bmatrix} \exp(-j\beta_{tq}z) \tag{18}$$

$$\begin{Bmatrix} F_{nm} \\ G_{nm} \end{Bmatrix} = \frac{1}{n_0 k_0} \left(\frac{n \mp 1}{r} \mp \frac{d}{dr} \right) \begin{Bmatrix} \Psi_{pq} \\ \Psi_{tq} \end{Bmatrix} \tag{19}$$

for the HE_{nm} modes (17) and for the EH_{nm} modes (18) where $Z = (n_0 Y_0)^{-1}$. These equations can be derived also by using (11) and (12) in this short paper and (27), (28), and (34) in [1]. Similarly, we obtain

$$\begin{Bmatrix} ZH_{z,0m} \\ E_{z,0m} \end{Bmatrix} \simeq -jG_{0m}(r) \exp(-j\beta_{1q}z) \tag{20}$$

for the TE_{0m}/TM_{0m} modes where G_{0m} is defined by the lower equation of (19) with $n = 0$. In Fig. 3 the radial functions F_{nm} and G_{nm} are compared with the z component of the electric field obtained by the numerical method [6], and good agreement is seen when the fiber is operated in the core mode region. In the Appendix the orthogonality relations of the vector modes are given.

VI. CONCLUSIONS

The relations between the scalar modes in a lenslike medium and the vector modes in a self-focusing optical fiber have been examined. By comparing the various propagation characteristics of the scalar modes with those of the vector modes obtained by the numerical method, and also by studying the field equations in a lenslike medium, it has been found that the vector modes in a self-focusing fiber with a finite homogeneous cladding can be adequately approximated by the scalar modes in an infinite lenslike medium when the fiber is operated in the core mode region where the normalized frequencies $k_0 a$ are large. Since the scalar modes can be expressed in terms of the analytical functions, they are in many situations more convenient to use. The present study also provides a means of identifying the scalar modes with the vector modes. However, outside the core mode region or for small values of $k_0 a$, the scalar-mode approximation yields propagation characteristics which are significantly different from those obtained by rigorous numerical methods. One should, therefore, exercise caution in using the scalar-mode approximation in connection with the study of integrated and fiber optics. A further point to notice is that both the scalar modes and the vector modes in a fiber with an infinite cladding cannot describe the cladding modes in the fiber with a finite cladding.

APPENDIX

The following orthogonality relations are easily verified by using (3), (4), and (14), and the orthogonality of the generalized Laguerre polynomials

$$\int_0^\infty \int_0^{2\pi} \begin{Bmatrix} E_{nm}^{HE} \cdot E_{n'm'}^{HE*} \\ E_{nm}^{EH} \cdot E_{n'm'}^{EH*} \end{Bmatrix} r dr d\theta = \delta_{nn'}\delta_{mm'} \tag{A1}$$

$$\int_0^\infty \int^{2\pi} \begin{Bmatrix} E_{0m}^{TE} \cdot E_{0m'}^{TE*} \\ E_{0m}^{TM} \cdot E_{0m'}^{TM*} \end{Bmatrix} r dr d\theta = \delta_{mm'} \tag{A2}$$

$$\int_0^{2\pi} E_{nm}^{HE} \cdot E_{n'm'}^{EH*} \, d\theta = 0 \tag{A3}$$

$$\int_0^{2\pi} E_{nm}^{HE} \cdot \begin{Bmatrix} E_{0m'}^{TE*} \\ E_{0m'}^{TM*} \end{Bmatrix} d\theta = 0 \tag{A4}$$

$$\int_0^{2\pi} E_{nm}^{EH} \cdot \begin{Bmatrix} E_{0m'}^{TE*} \\ E_{0m'}^{TM*} \end{Bmatrix} d\theta = 0 \tag{A5}$$

$$E_{0m}^{TE} \cdot E_{0m'}^{TM*} = 0 \tag{A6}$$

where the asterisk (*) denotes a complex conjugate, δ_{ij} is the Kronecker delta, and (A3)–(A6) hold even if the asterisk is dropped.

ACKNOWLEDGMENT

The authors wish to thank Dr. C. N. Kurtz of the Eastman Kodak Company for his useful comments.

REFERENCES

[1] C. N. Kurtz and W. Streifer, "Guided waves in inhomogeneous focusing media. Part I: Formulation, solution for quadratic inhomogeneity," *IEEE Trans. Microwave Theory Tech.*, vol. MTT-17, pp. 11–15, Jan. 1969.
[2] H. Kirchhoff, "Wave propagation along radially inhomogeneous glass fibres," *Arch. Elek. Übertragung*, vol. 27, pp. 13–18, Jan. 1973.
[3] P. J. B. Clarricoats and K. B. Chan, "Electromagnetic wave propagation along radially inhomogeneous dielectric cylinders," *Electron. Lett.*, vol. 6, pp. 694–695, Oct. 1970.
[4] G. L. Yip and Y. H. Ahmew, "Propagation characteristics of a radially inhomogeneous optical fibre," *Electron. Lett.*, vol. 10, pp. 37–38, Feb. 1974.
[5] A. Vigants, "Propagation of electromagnetic surface waves along cylindrical columns with arbitrary radial permittivity variation," Columbia Univ., New York, N. Y., Tech. Rep. 69, 1961.
[6] Y. H. Ahmew, "Propagation characteristics of the self-focusing fiber waveguide," M.S. thesis, McGill Univ., Montreal, Canada, Aug. 1973.
[7] W. Streifer and C. N. Kurtz, "Scalar analysis of radially inhomogeneous guiding media," *J. Opt. Soc. Amer.*, vol. 57, pp. 779–786, June 1967.
[8] S. Kawakami and J. Nishizawa, "An optical waveguide with the optimum distribution of the refractive index with reference to waveform distortion," *IEEE Trans. Microwave Theory Tech.*, vol. MTT-16, pp. 814–818, Oct. 1968.
[9] D. Marcuse, "The impulse response of an optical fiber with parabolic index profile," *Bell Syst. Tech. J.*, vol. 57, pp. 1169–1174, Sept. 1973.
[10] E. Snitzer, "Cylindrical dielectric waveguide modes," *J. Opt Soc. Amer.*, vol. 51, pp. 491–498, May 1961.
[11] C. N. Kurtz, private communication.